

VICTORIA UNIVERSITY
MELBOURNE AUSTRALIA

Improving the moisture barrier and mechanical properties of semi-refined carrageenan films

This is the Published version of the following publication

Sedayu, Bakti B, Cran, Marlene and Bigger, Stephen W (2020) Improving the moisture barrier and mechanical properties of semi-refined carrageenan films. *Journal of Applied Polymer Science*, 137 (41). ISSN 0021-8995 (print), 1097-4628 (online)

The publisher's official version can be found at
<https://onlinelibrary.wiley.com/doi/full/10.1002/app.49238>
Note that access to this version may require subscription.

Downloaded from VU Research Repository <https://vuir.vu.edu.au/41212/>



Improving the moisture barrier and mechanical properties of semi-refined carrageenan films

Bakti B. Sedayu^{1,2} | Marlene J. Cran¹ | Stephen W. Bigger¹

¹Institute for Sustainable Industries and Liveable Cities, Victoria University, Melbourne, Australia

²Agency for Marine and Fisheries Research and Development, Republic of Indonesia. Jl. Pasir Putih II, Ancol Timur, Jakarta Utara, Indonesia

Correspondence

Marlene J. Cran, Institute for Sustainable Industries and Liveable Cities, Victoria University, PO Box 14428, Melbourne 8001, Australia.

Email: marlene.cran@vu.edu.au

Abstract

Semi-refined carrageenan (SRC) films are sensitive to moisture and generally have poor mechanical properties. These factors limit their use in applications where moisture levels are high and good mechanical strength is required. This work investigated the incorporation of nanoclay (NC) into SRC film in combination with surface lamination using a thin layer of poly(caprolactone) (PCL) to enhance the barrier properties and hydrophobicity of the SRC film and concurrently improved the mechanical properties. The water vapor permeability, moisture uptake, and water solubility decreased by 92, 24, and 11%, respectively, and the water contact angle increased from 72° to 95°. The tensile strength and elongation at break increased by 17.9 and 2.8%, respectively, and the thermal stability also increased slightly. The PCL lamination was the main contributor to the enhanced barrier and mechanical properties of the films, whereas the NC inclusion contributed more to the enhanced thermal properties.

1 | INTRODUCTION

An increasing trend in the use of eco-friendly plastics over recent years has resulted in intensive research into new biomaterials that can be used as substitutes for conventional synthetic polymers.^[1] Among these alternative biomaterials, seaweed-derived bioplastics such as carrageenans have gained increasing attention, particularly in food packaging applications.^[2–4] This is mainly due to the environmental sustainability, low cost, and the ethical considerations associated with competition with terrestrial crops for human food.^[5] Two different grades of carrageenan are typically used for the production of films and these differ by the degree of refinement applied during the extraction from the seaweed matrix. Semi-refined carrageenan (SRC) is subjected to fewer refinement steps and thus contains some residual impurities whereas in

refined carrageenan, most of the impurities are removed. Regardless of the grade of carrageenan used, the hydrophilic nature of films produced from this material imposes some limitations on their performance in applications where they are exposed to moisture or water.^[6,7]

Hydrophilicity can pose a critical problem in food packaging applications since the major quality losses of packaged foods are associated with water vapor and gas transfer through packaging films.^[8] In addition, the inability of these materials to accommodate high water content produce such as meats, fruits, and liquid products severely constrains their implementation in the packaging of these food items. Plasticizers are usually incorporated into carrageenan polymers to obtain desirable mechanical properties because films comprised entirely of carrageenan are inherently brittle.^[9,10] Nonetheless, the addition of plasticizers is also well known to

This is an open access article under the terms of the Creative Commons Attribution License, which permits use, distribution and reproduction in any medium, provided the original work is properly cited.

© 2020 The Authors. *Journal of Applied Polymer Science* published by Wiley Periodicals, Inc.

exacerbate the moisture sensitivity of polysaccharide films.^[11,12] To address this and other drawbacks, reinforcing nanoclays (NCs) and blending of hydrophobic materials into carrageenan-based film have been studied and have demonstrated positive outcomes.^[13–15]

The inclusion of natural NCs into bio-based polymers has been reported to successfully enhance the barrier and mechanical properties of the produced films.^[13,16,17] Although hydrophilic NCs may increase the water sensitivity of bio-based films, they are more compatible with such polymers than hydrophobic NCs and can therefore form a highly even dispersion (intercalation) within the matrix.^[18] The enhanced barrier properties can be explained by the tortuous conformation of the clay particles that obstruct the penetration of moisture or oxygen passage through the films.^[16,19] In addition to this, Müller et al.^[20] have also observed that bio-based films containing a hydrophobic type of NC have inferior water vapor and mechanical properties compared with those that contain a hydrophilic clay.

The incompatibility of hydrophilic polymers in blends with hydrophobic substances has been a major constraint in obtaining desirable products.^[21] This often results in poor dispersion within the mixture, and consequently brings undesirable impacts to the films that are produced such as agglomeration, poor optical properties, and/or poor mechanical properties.^[22–24] With regard to the latter, the mechanical property requirements of a given packaging material depend on its specific application. For example, semi-rigid food containers, in general, do not require high elongation properties but need higher tensile strength (TS) to ensure the structural integrity. In the case of films, stretchability or high elongation at break (EB) is often required, particularly in the case of stretch-wrap films.^[25]

An alternative to blending that can potentially achieve better outcomes is layering or lamination of hydrophilic films with a hydrophobic substance.^[26] Examples of common bilayer products that are readily found in the global market include takeaway paper coffee cups and food containers where a hydrophobic layer (polymer film) is applied to be in contact with the food product with this layer able to withstand water or high moisture levels. The current barrier materials used in layering biodegradable packaging films commonly originate from synthetic polymers such as poly(vinyl alcohol), polyethylene, fluorocarbon polymers, or ethylene vinyl alcohol copolymers.^[27,28] Using such materials may bring disadvantages in terms of their ecological aspects because they are not readily biodegradable^[29] and may not be recycled due to difficulty in separating the layers.^[30] Poly(caprolactone) (PCL), an aliphatic polyester, is a

commercially available synthetic biodegradable polymer with a crystallinity of around 50% and a low melting point of 60°C.^[31,32] Duarte et al.^[33] used PCL as a barrier layer for polysaccharide-based film and found the laminates to be environmentally biodegradable. Poly(caprolactone) also has high flexibility and films prepared by heat press-molding have shown a TS of 33 MPa and an EB of more than 1,100%.^[34] Increase in the mechanical strength of pea starch films has also been reported upon the incorporation of PCL.^[35,36]

In view of the desirable environmental and economic benefits of using SRC as a substrate for food packaging polymer systems, the current article investigated the possible enhancement of its hydrophobicity as well as its barrier and physicomechanical properties by the incorporation of nanoclay (NC) in combination with surface lamination using a thin layer of PCL. It is envisaged that an improvement in these properties of SRC would enable its use as a packaging material for high moisture-containing foods in particular.

2 | EXPERIMENTAL

2.1 | Materials

SRC (E407a) derived from *Eucheuma cottonii* seaweed was purchased from W-Hydrocolloids, Inc. (the Philippines). The properties of the SRC include: powder size <89 μm, moisture content of 12% (w/w), pH 8–11, average water gel strength at 1.5% (w/v)/20°C of 300 g cm⁻², average potassium gel strength at 1% (w/v)/20°C of 400 g cm⁻².

Typically, carrageenan derived from *E. cottonii* seaweed has an average molecular weight (MW) of ca. 614 kDa, and a composition of 50.1 mol% galactose, 43.6 mol% 3,6-anhydro-galactose, 4.3 mol% glucose, 0.9 mol% 6/4/0-O-methylgalactose, 0.9 mol% xylose, and 0.2 mol% mannose.^[37] The maximum levels of heavy metal impurities Pb, As, Hg, and Cd are 5, 3, 1, and 2 ppm, respectively. The total amount of rough impurities after filtration through Grade 4 Whatman filter paper is ca. 21% (w/w), comprised mainly of residual cellulose and other elements.^[37] Hydrophilic bentonite nanoclay (MW = 180.1 g mol⁻¹), PCL (MW = ca.14 kDa), glycerol, and KNO₃ (≥ 99.0%) were purchased from Sigma-Aldrich, Australia. The choice of a hydrophilic NC was made in order to achieve a high dispersion of the clay particles within the matrix of the polymer. Milli-Q water was used as a solvent for the SRC and NC, whereas tetrahydrofuran (THF, ≥99.0%, Sigma Aldrich, Australia) and Mg(NO₃)₂ (Ajax Finechem, Australia) were used as a solvent in the preparation of PCL and conditioning of the samples.

2.2 | Film preparation

A solvent casting method was used in the preparation of SRC films^[11] whereby 5 g of SRC was dissolved in 250 ml of deionized water at 22°C with vigorous stirring for 15 min to remove SRC agglomerates. Afterward, the solution was heated and maintained under stirring at 90°C for 30 min before the plasticizing agent glycerol (2 g) was added. The solution was then cooled for around 5 min to remove bubbles or foam before it was poured evenly onto rectangular acrylic casting trays (200 × 150 × 3 mm). The film was allowed to dry at 22°C in a fume hood for 36 hr before it was peeled away from the tray.

A second preparation of NC-reinforced SRC film (SRC/NC) was performed using the method proposed by Rhim^[38] with some modifications. Relative to SRC, a solution of 6% (w/w) hydrophilic bentonite NC was dispersed/swollen in 150 ml of water with constant stirring for 24 hr at 45–50°C. The NC solution was then sheared at 20,000 rpm using a homogenizer (CAT Unidrive × 1000, Germany) for 10 min, followed by a further 10 min of sonication at 80% amplitude and 50 Hz. Separately, 5 g of SRC in 100 ml was prepared as described above and both solutions were then mixed and stirred for 15 min followed by heating at 90°C for 30 min. The glycerol addition and casting procedure were similar to that used in the preparation of the SRC film (see above). The selection of 6% (w/w) NC was based on a screening process whereby different levels of NC were added and the TS tested (see Figure S1 in Supplementary Material). A level of 6% (w/w) NC showed the greatest improvement with higher levels resulting in lower TS values.

A third preparation of SRC and NC reinforced films laminated with PCL (SRC/NC/PCL) was obtained by pouring a 6% (w/w) PCL solution dissolved in THF onto the upper surface of the SRC/NC films. The PCL solution was poured evenly onto the surface of the dried films, and the excess solution was immediately removed from the film by holding the tray upright before the films were left to dry at 22°C.

2.3 | Film conditioning and thickness

Prior to characterization testing and measurement, all film samples were conditioned for 48 hr at 22°C in a desiccator containing saturated Mg(NO₃)₂ solution to obtain a 53% RH environment. The thickness of each sample was measured using a digital micrometer (Schut IP54, The Netherlands) with a 0.001 mm precision. The thickness measurements were used in the calculations of the water vapor permeability and mechanical property parameters.

2.4 | Barrier properties and water resistance

2.4.1 | Moisture content

The moisture content of the films was measured by drying rectangular film samples (2 × 2 cm) in an air-circulating oven at 105°C, until a constant dry weight of each film was obtained.^[39]

2.4.2 | Water vapor permeability

The water vapor permeability (WVP) measurements were made using a method by Sobral et al.^[40] Circular film samples were placed on the lid of a permeation cup containing silica gel to achieve 0% RH inside the cup. To ensure adequate sealing, Vaseline was applied evenly between the lip of the cup and its lid. The cups were then placed on a tray in a desiccator under a saturated humidity environment (100% RH) that was created by adding water in the base of the desiccator, ensuring that the cups were not in direct contact with the water. The desiccator was maintained at 22°C, and the mass of each sample cup was measured at 24-hr intervals for 7 days. The WVP was calculated using the following equation:

$$\text{WVP} = \left(\frac{w}{tA} \right) \times \left(\frac{x}{\Delta P} \right) \quad (1)$$

where w is the mass of the sample cup at time t , A is the exposed area of the film (cm²), x is the thickness of the film (mm), and ΔP is the difference in the partial pressures of water vapor (Pa) existing across the film. The ratio w/t was calculated from the slope of the mass gain versus time plot.

2.4.3 | Water contact angle

The water contact angle (WCA) was measured to observe the hydrophobicity or wettability of the film surface using a drop shape analyzer (Kruss DSA30S, Germany). To achieve a flat surface during measurement, each film sample was glued to the top of a glass slide and a 4 μl water droplet was placed onto the surface of the film using a micro-syringe. The PCL-layered surface of the bilayer films was placed facing upwards against the water droplet. The angle between the horizontal baseline of the water droplet and the tangent at the droplet boundary was measured using Advance 1.6.1.0 software. At least 10 measurements of each sample were taken at random surface positions on the substrate to obtain the average.

2.4.4 | Moisture uptake

The moisture uptake of the films was measured gravimetrically using a method in accordance with Rhim and Wang.^[14] Prior to the moisture sorption process, the film samples (50 mm × 25 mm) were dehydrated at 60°C in an oven for 48 hr. The samples were weighed using an analytical balance with a precision of 0.0001 g and were immediately placed in a desiccator containing a saturated solution of KNO₃ to obtain a 98% RH environment. The desiccator was then placed in an incubator at 25°C for 24 hr after which the moisture uptake was calculated based on the percentage mass gain compared to the original mass of the sample.

2.4.5 | Film solubility

A modified method by Rhim and Wang^[14] was used to evaluate the water solubility (WS) of the film samples. Square samples of film (12.7 mm²) were first dried at 105°C in an oven for 24 hr to determine their initial dry mass. Each sample was placed in a 50 ml centrifuge tube containing 30 ml of water and then capped. The tubes were immediately placed in a 25°C shaker water bath (Ratek SWB20D, Australia) for 30 min with constant, gentle shaking. The mass of each undissolved, dry film was determined by taking the remaining pieces of the samples from the tube and gently blotting the wet surface with absorbent tissue before drying in an oven at 105°C for 24 hr. The WS of the film was calculated as the percentage ratio of the mass of soluble matter to the initial mass of the sample:

$$WS = \frac{W_O - W_F}{W_O} \times 100 \quad (2)$$

where W_O is the initial mass of the dried film, and W_F is the mass of the final undissolved film.

2.5 | Mechanical properties

The mechanical properties of the SRC film samples were measured in accordance with ASTM Method D882.^[41] The measurements were made using an Instron Universal Testing Machine (Model 4301) coupled with a 5 kN load cell with at least eight strip of film (100 mm × 15 mm) taken from each sample to obtain an average value for each of the properties. An initial separation between the grips of 50 mm, at a cross-head speed of 10 mm min⁻¹, was used.^[24] The mechanical properties were evaluated based on the resulting stress-strain curves using BlueHill

Series IX software to obtain the TS, EB, and elastic modulus (EM).

2.6 | Color and optical properties

The surface color of the film samples was determined using a chroma-meter (Konica Minolta CR-400, Japan) which measured the lightness (L^*), redness/greenness (a^*), and yellowness/blueness (b^*) parameters. Average values were calculated from data taken at three random positions on the film surface that were tested in triplicate. A standard white plate ($L^* = 97.39$, $a^* = 0.03$, and $b^* = 1.77$) was used for calibration and as the base for the films during measurement.

A UV-visible spectrophotometer (Biochrom Libra S12) was used to evaluate the opacity of each film sample by measuring the optical absorbance of the film at $\lambda = 550$ nm. Three specimens (14 mm × 12.5 mm) were selected from different locations on the film samples and tested following the method by Gómez-Estaca et al.^[42] with slight modification. The film samples were placed directly into the test cell of the spectrophotometer and an empty cell was used as the reference. For the laminated film samples, the PCL-layered surface was placed facing toward the light source for consistency with regard to any differences in light scattering between the two layers. The opacity was calculated using the equation^[13]:

$$Op = A_{550}/x \quad (3)$$

where Op is the opacity, A_{550} is the absorbance of the film at $\lambda = 550$ nm, and x is the thickness of the film sample (mm).

2.7 | Thermal analysis

The thermal stability of each film sample was investigated by thermogravimetric analysis (TGA) using a Mettler-Toledo TGA/DSC1 thermal analyzer (Mettler-Toledo, Schwarzenbach, Switzerland). Samples weighing 8–12 mg were placed in an alumina crucible and were heated from 30 to 400°C at a heating rate of 10°C min⁻¹. Nitrogen at a flow rate of 20 ml min⁻¹ was used as the purge gas during the heating.

2.8 | Structural analysis

Fourier-transform infrared (FTIR) spectra of the films were recorded using a Perkin-Elmer Frontier FTIR spectrophotometer (PerkinElmer, Inc., Waltham, Massachusetts, USA)

equipped with a diamond crystal attenuated total reflectance (ATR) accessory. A small piece of film sample was clamped onto the ATR crystal and the spectral transmittance was measured within the range 4,000–600 cm^{-1} using an average of 64 scans, at 4 cm^{-1} resolution. For the laminated film specimens, the surface of the PCL layer was placed in contact with the ATR crystal. Data processing was performed using Perkin-Elmer Spectrum 10 software.

2.9 | Scanning electron microscopy

Small sections of film samples were adhered to aluminum stubs using double-sided conductive carbon tape and were then coated with iridium using a sputter coater (Cressington, UK). In the case of the laminated films, the PCL-layered surface was observed. Imaging of the surfaces of the films and cross-section analyses were conducted using a Hitachi Tabletop (TM 3030 Plus) scanning electron microscope (SEM) equipped with an energy dispersive X-ray (EDX) spectrometer. To observe the NC dispersion within the matrix of the film, silica spectra were produced by EDX mapping using AztechOne software (Oxford Instruments, UK).

2.10 | Statistical analysis

Statistical analyses of the experimental data were conducted using IBM-SPSS Statistics 24 software. One-way analysis of variance (ANOVA) was performed and the significance among the mean values of sample properties was determined with the Duncan test at a 5% significance level.

3 | RESULTS AND DISCUSSION

3.1 | Morphological and physical properties

The film samples were relatively uniform in thickness and were flexible with a yellowish translucent surface. As

expected, the addition of NC slightly increased the film thickness from 0.66 to 0.69 mm (see Table 1) with similar results reported by Shojaee-Aliabadi et al.^[13] and Rhim and Wang^[14] for κ -carrageenan films. Interestingly, the PCL-layered SRC films showed a negligible change in thickness in comparison with the unlayered films, thus indicating the formed PCL layer was very thin.

Figure 1a shows the cross-sectional image of a laminated SRC/PCL film where the PCL layer is 2–3 μm thick. There is also no visible delamination (see Figure 1a) indicating strong interfacial adhesion between the SRC and PCL film layers. This adhesion may be initiated by hydrogen bonding interactions between the carbonyl groups of the PCL and the hydroxyl groups of the SRC and/or the plasticizer (glycerol). Similar hydrogen bonding between PCL and polysaccharides has been reported previously by Honma et al.^[43]

The surface image of the SRC film (Figure 1b) shows some segregated domains as well as the presence of aggregated particles. These particles are mainly impurities commonly found in the raw SRC such as cellulosic residues. The inclusion of NC in SRC film formulation resulted in a rougher surface but with smaller domains than those of the SRC film and irregular surface aggregates (see Figure 1c). Impurities present in raw SRC may interact with the NC particles during film preparation and consequently cause agglomeration. These aggregates may further impact upon the final physical-mechanical, and barrier properties of the film.

In the case of the PCL laminated films, both the SRC/PCL and SRC/NC/PCL films display similar surface images as shown in Figure 1d,e, respectively. In the case of the SRC films containing NC, larger, more regular domains are observed compared with the neat SRC film, thus making the surface appear smoother. The smoothness of the surface is affected by the presence of NC in the matrix that facilitates a rougher surface contour thereby producing a stronger bond between the SRC and PCL film surfaces. Additionally, the surface smoothness might also be affected by the interaction between the hydrophilic clay particles on the film surface with the PCL polymer, which creates a more compatible interfacial adhesion between the layers. Such a phenomenon

TABLE 1 Physical properties of the SRC/NC/PCL film formulations

Film samples	Thickness (mm)	Moisture content (%)	L^*	a^*	b^*	Opacity
SRC	0.066 ± 0.001 ^a	25.90 ± 0.76 ^a	88.22 ± 0.15 ^a	0.12 ± 0.04 ^a	7.57 ± 0.21 ^a	12.45 ± 0.37 ^a
SRC/NC	0.069 ± 0.001 ^c	23.87 ± 0.61 ^b	86.90 ± 0.18 ^b	0.21 ± 0.03 ^b	9.68 ± 0.18 ^b	13.67 ± 0.29 ^b
SRC/PCL	0.066 ± 0.002 ^{ab}	23.62 ± 0.72 ^b	88.32 ± 0.32 ^a	0.16 ± 0.03 ^c	6.96 ± 0.32 ^c	10.86 ± 0.37 ^c
SRC/NC/PCL	0.068 ± 0.002 ^{bc}	22.94 ± 0.94 ^b	87.31 ± 0.20 ^c	0.16 ± 0.03 ^c	8.86 ± 0.39 ^d	13.13 ± 0.59 ^d

Note: Values are given as mean with one SD. Any two means in the same column followed by the same letter are not significantly different ($p > .05$) as determined by a Duncan's test.

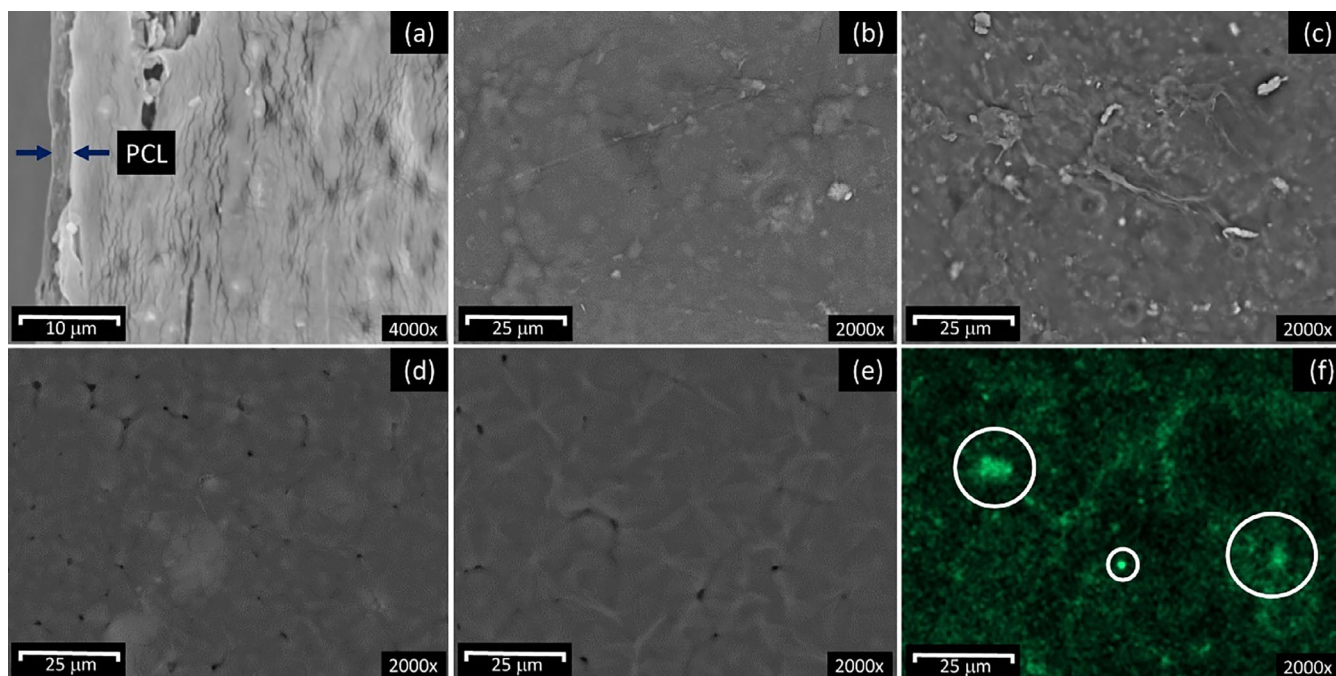


FIGURE 1 Scanning electron micrographs and EDX images of SRC/NC/PCL film formulations: (a) cross-sectional image of SRC/PCL, (b) SRC, (c) SRC/NC, (d) SRC/PCL, and (e) SRC/NC/PCL film; (f) EDX image of Si dispersion in SRC/NC film based on image (c). The aggregation of some of the NC particles is indicated by the circles in image (f). Color image available online [Color figure can be viewed at wileyonlinelibrary.com]

has also been reported by Eng et al.^[44] in an investigation of hydrophilic clay/PCL blends.

The incorporation of the hydrophilic NC in the SRC film formulation resulted in greater homogenous dispersion in comparison with a less hydrophilic type of NC (see Figure S2 in the Supplementary Material). The dispersion of NC particles represented by the silica elemental distribution showed a relatively even dispersion over the surface of the SRC film shown in Figure 1f. However, some clay particle aggregates are also identified within the matrix and this aggregation might be caused by an excessive concentration of NC in the matrix of the SRC. Even though the addition of 6% (w/w) of NC into SRC produces a film with optimum mechanical strength, this concentration may have facilitated agglomeration.

Table 1 lists the film thickness, moisture content, color, and opacity of the SRC film samples. Many of these properties are important considerations for packaging films and are particularly related to consumer acceptance. The data suggest that the moisture content of SRC films is significantly decreased ($p < .05$) by the inclusion of NC as well as by PCL lamination. This behavior may be explained by a reduction in the amount of available hydroxyl groups in the structure of the SRC film that can interact with water since these groups also interact with the clay particles^[13] and PCL molecules.

The incorporation of the NC into the matrix of the SRC polymer increased the opacity of the film due to the dispersion of particles through the matrix obstructing the transmission of light.^[45] The thickness of the SRC and SRC/PCL-laminated films is similar (see Table 1) and the optical density of the SRC is much greater than that of the PCL. Whence the observed opacity difference between these two films may be explained by the effective decrease in the optical path length of light through the more optically dense SRC medium that is achieved upon lamination.

The surface color of the SRC film was affected by the NC incorporation and the lamination with PCL. The incorporation of NC into the SRC resulted in a significant decrease in the lightness (L^*), redness/greenness (a^*), and yellowness/blueness (b^*) values, whereas lamination of SRC with PCL resulted in no significant change in the lightness but an increase in the a^* value and decrease in the b^* value (see Table 1). The decrease in lightness may be a result of the NC incorporation into the SRC polymer matrix rendering a matte finish to the film surface and a subsequent enhancement of the natural yellowish tint of SRC film. Similar observations of increased yellowness were also observed in alginate and whey protein isolate nanocomposite films reinforced with hydrophilic montmorillonite clay.^[46,47] In comparison with clear transparent films obtained using refined carrageenan, the

yellowish appearance of SRC films may originate from residual substances including glucan, insoluble aromatic compounds, and minerals.^[48]

3.2 | Moisture barrier properties and hydrophobicity

Moisture barrier properties are among the more important properties that must be considered when developing films for food packaging applications. The WVP of any polymeric film, for example, depends on the chemical conformation and morphology of the polymer matrix, the nature of the permeant film, and the temperature of the surrounding environment.^[49]

The WVP, moisture uptake, WCA, and WS values of the different SRC film samples are shown in Table 2. The results suggest that the WVP of the SRC substrate is increased slightly upon the addition of NC to the formulation but is considerably decreased, as expected, by the addition of the PCL layer. In the case of the SRC/NC film, the lack of improvement in WVP may be due to the heterogeneous dispersion of the NC particles within the matrix since some agglomeration occurs as described above. This can lead to a less effective barrier to water vapor transmission through the matrix. The results also suggest that the hydrophobicity of the films increases upon addition of NC and lamination of the SRC as indicated by the lower moisture uptake values.

The WCA values indicate a slight decrease in hydrophobicity occur upon the addition of NC to the SRC possibly due to surface effects (see Figure 1c) caused by the impurities in the formulation and which facilitate a higher interfacial adhesion between the film surface and the water drop. However, this effect is very much compensated for by the PCL lamination of the SRC where a considerable increase in the WCA values is observed.

The WS values also reflect the resistance of the film formulation to water that may be present on the surface of foods when the film is applied as a food packaging medium, and may also reflect its inherent

biodegradability.^[50] Also shown in Table 2, the WS value was slightly increased respectively upon the incorporation of the NC into the SRC film. This may be a result of the inclusion of the hydrophilic NC rendering the film to be more readily degraded in water. Similar behavior has also been reported by Alboofetileh et al.^[46] in alginate films prepared using hydrophilic montmorillonite clay.

The seemingly unexpected decrease in the moisture uptake from 49 to 45% that was observed when a hydrophilic additive such as bentonite was added to the matrix of the SRC can possibly be explained by an interaction between the clay particles with SRC and glycerol in the formulation. This occurs through ion–dipole interactions between sodium ions in the NC and the hydroxyl groups from the SRC and glycerol that reduce the availability of hydroxyl groups that are capable of interacting with surrounding water molecules. The overall effect thereby results in a less hygroscopic film.^[51]

The addition of NC alone did not alter the WVP considerably; however, layering the films with PCL generally improved the moisture barrier and surface hydrophobicity. The PCL layer reduced the WVP and WS values by ca. 19 and 10%, respectively, for the SRC/PCL samples compared with the SRC samples and by ca. 22 and 17%, respectively, for the SRC/NC/PCL compared with SRC/NC films. The PCL layer also increased the WCA values of the SRC and SRC/NC films to a value greater than 95° (see Table 2). The enhancement of the water barrier properties of the films would be beneficial in protecting packaged foods affected by moisture content or high water activity.^[52] The overall moisture barrier and water resistance improvement provided by the PCL layer can be associated with its hydrophobic characteristics that protect the SRC or SRC/NC film surface from direct contact with any surrounding water. Moreover, the PCL layer may reduce the number of hydroxyl functional groups per unit volume or area in the SRC films that are able to interact with water molecules from the environment.^[35] The results of the present study are consistent with the negligible moisture or water sorption reported for other PCL-based films.^[29,53]

TABLE 2 Barrier properties and hydrophobicity of the SRC/NC/PCL film formulations

Film samples	WVP (g mm cm ⁻² hr ⁻¹ pa ⁻¹) (× 10 ⁻⁷)	Moisture uptake (%)	WCA (degree)	WS (%)
SRC	10.47 ± 0.09 ^a	49.07 ± 2.12 ^a	72.17 ± 3.98 ^a	49.12 ± 2.26 ^a
SRC/NC	10.67 ± 0.03 ^a	44.90 ± 1.55 ^b	69.77 ± 3.79 ^b	49.65 ± 1.80 ^b
SRC/PCL	8.43 ± 0.45 ^b	44.21 ± 1.15 ^b	95.78 ± 2.82 ^c	46.86 ± 0.97 ^{ac}
SRC/NC/PCL	8.36 ± 0.48 ^b	37.21 ± 1.84 ^c	95.20 ± 2.45 ^c	43.73 ± 3.76 ^c

Note: Values are given as mean with one SD. Any two means in the same column followed by the same letter are not significantly different ($p > .05$) as determined by a Duncan's test.

3.3 | Mechanical properties

The mechanical properties of the film samples, namely the TS, EM, and EB results, are shown in Figure 2. The incorporation of NC into the matrix of the SRC matrix had no significant effect on the TS but increased the EM with a corresponding decrease in the EB value. The incorporation of NC in the SRC increased the EM of the film by 18.6% whereas the EB was decreased by 17.2%. The increased value of EM can be associated with the interactions between the polymer matrix and intercalated

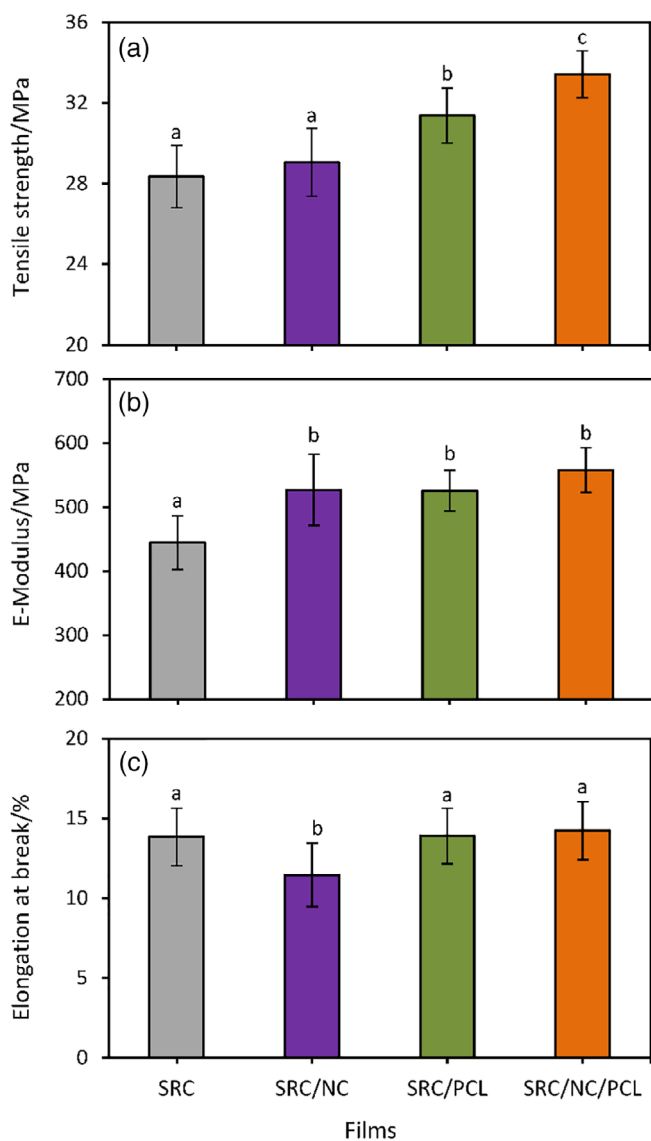


FIGURE 2 TS, EB, and EM of SRC/NC/PCL film formulations measured in accordance with ASTM Method D882. Error bars represent the SD calculated at the 95% level of confidence. The same letters above data bars indicate no significant difference in the values as determined by a Duncan's test (i.e., $p > .05$). Color image available online [Color figure can be viewed at wileyonlinelibrary.com]

clay particles resulting in a high aspect ratio and high surface area through hydrogen bonds.^[54,55] The reduction in EB is attributed to the decreasing moisture content in the SRC/NC film. Since water molecules plasticize the SRC polymer matrix, decreasing the water content will consequently increase the stiffness, and thus decrease the EB.^[51,56,57]

The PCL lamination of the SRC film increased the TS and EM by 10.7 and 18.3%, respectively, but had no significant effect on the EB. Moreover, the combination of both NC reinforcement and PCL lamination ultimately contributed to the highest enhancement in both the TS and EM of the SRC film with respective increases in these mechanical properties of 17.9 and 25.6%. There appears to be a slight (2.8%) increase in the EB value however this difference was found to be statistically insignificant compared to the SRC control sample.

3.4 | Thermal properties

The TGA provides information about the effect of NC incorporation and PLA lamination on the thermal stability of the films. As shown in Figure 3, the mass loss during thermal degradation for each of the films exhibited similar behavior with three major stages of decomposition. The initial decomposition occurred between 50 and 120°C with small, broad peaks (see the derivative, dTGA curves) that correspond to the evaporation of bonded water within the films. The second mass loss step occurred between 170 and 240°C and corresponds to the volatilization of the glycerol plasticizer from the polymer.^[38] The third and final step occurred at ca. 260°C and is attributed to the decomposition of the SRC polymer chains as well as the commencement of the PCL layer decomposition, which begins at 265°C.

As displayed in Figure 3, both NC inclusion and PCL lamination resulted in an increase in the thermal stability of the SRC films with smaller mass losses observed than those of the SRC control film. Furthermore, the incorporation of NC imparted a slightly higher stability than PCL lamination, particularly during the first and second stages of degradation. The migration of water, plasticizer, and/or other volatilized compounds may be retarded by the dispersed clay within the matrix due to the thermal insulation properties of the clay, as well as the tortuous pathway introduced by the NC platelets that can inhibit the exudation of the molecules from the matrix.^[58] Similar results have also been reported by Kumar et al.^[59] who found a significant delay in the mass loss of soy protein isolate films reinforced with NC during thermal degradation.

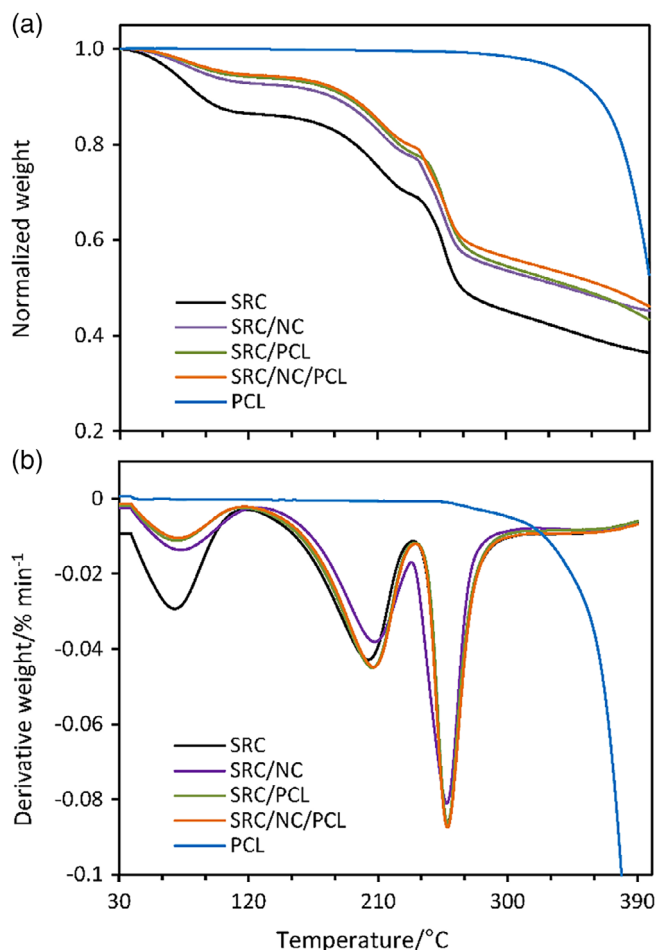


FIGURE 3 Thermograms of SRC/NC/PCL film formulations: (a) TGA thermogram and (b) derivative dTGA thermogram. Samples were heated under nitrogen (flow rate 20 ml min⁻¹) at a heating rate of 10°C min⁻¹. Color image available online [Color figure can be viewed at wileyonlinelibrary.com]

The DSC thermograms in Figure 4 demonstrate that the incorporation of NC increased the glass transition temperature (T_g) of the SRC from 133 to 163°C that is also associated with the melting temperature of the polymer, whereas the presence of the PCL layer had little effect on the T_g of the SRC substrate. The relatively sharp exothermic peak at 222°C observed in Figure 4a,b,d is attributed to the decomposition temperature of the SRC substrate and/or glycerol component^[11] which is less intense in the case of the PCL-laminated SRC sample (Figure 4c). At temperatures greater than 222°C, convoluted peaks attributed to the incipient stage of the decomposition of the main SRC polymers are visible with a more intense peak observable at 265°C which is consistent with the TGA data (see Figure 3). The intensity of the peak at 265°C is reduced in the presence of the NC confirming the results of the TGA experiments that suggest the NC may stabilize the substrate to some extent.

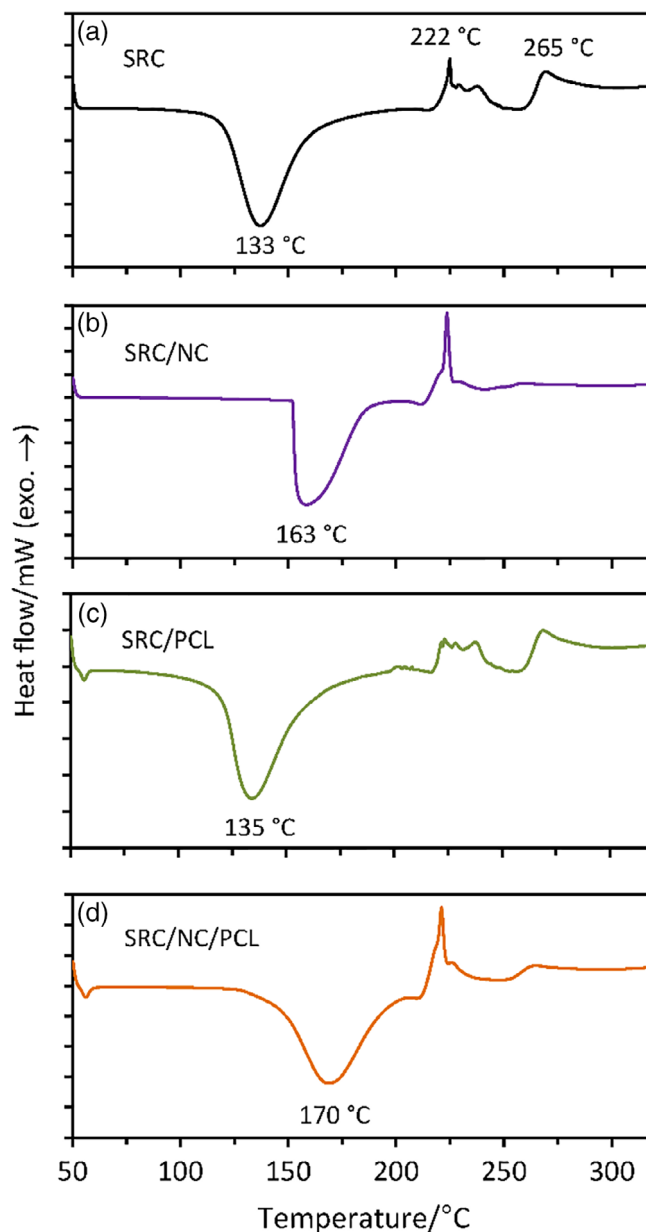


FIGURE 4 The DSC thermograms of SRC/NC/PCL film formulations: (a) SRC, (b) SRC/NC, (c) SRC/PCL, and (d) SRC/NC/PCL. Samples were heated under nitrogen (flow rate 20 ml min⁻¹) at a heating rate of 10°C min⁻¹. Color image available online [Color figure can be viewed at wileyonlinelibrary.com]

Moreover, the PCL layer began to melt at ca. 60°C and this molten polymer may subsequently protect the SRC films during further heating that indirectly leads to an increase in the thermal stability of the SRC film.

3.5 | Structural properties

FTIR spectra were obtained to investigate the interaction between the SRC film, NC particles, and the PCL layer.

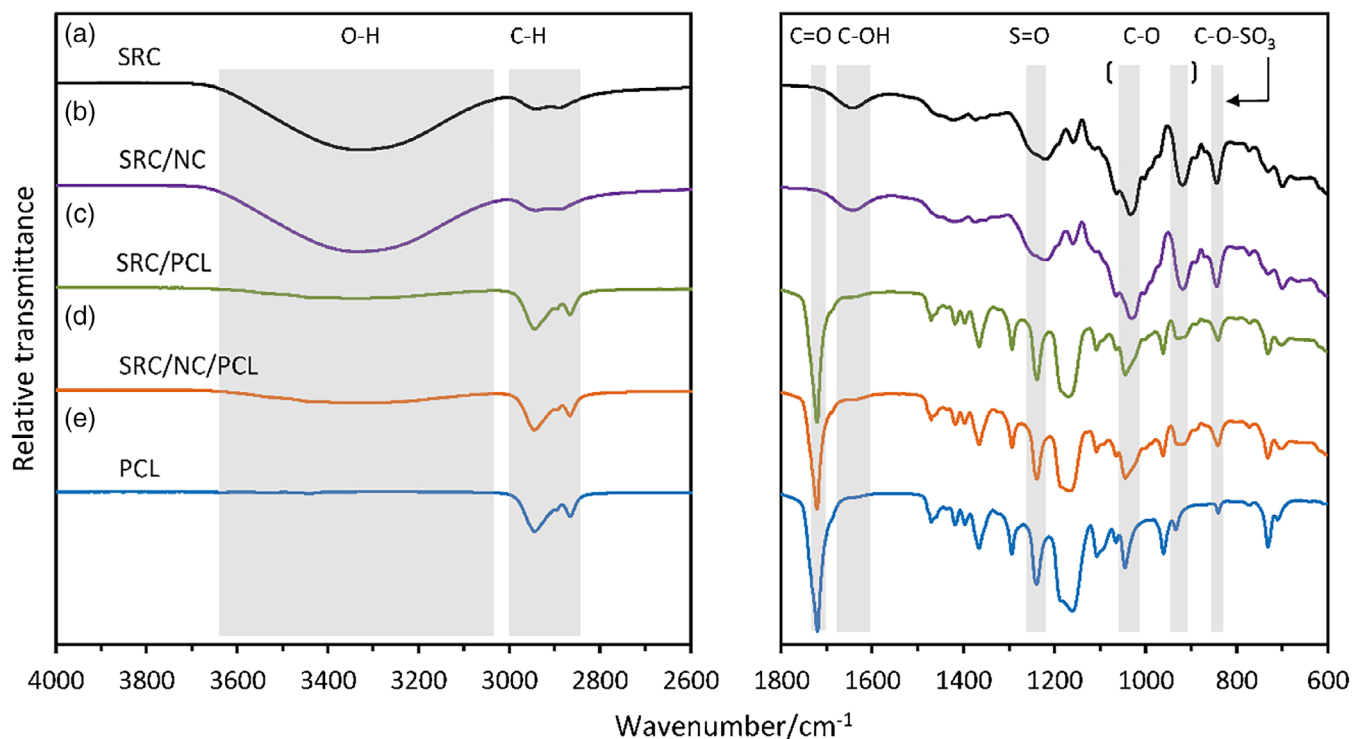


FIGURE 5 FTIR spectra of SRC/NC/PCL film formulations: (a) SRC, (b) SRC/NC, (c) SRC/PCL, (d) SRC/NC/PCL, and (e) PCL. Spectra were recorded using an average of 64 scans at 4 cm^{-1} resolution. For the laminated film specimens, the surface of the PCL layer was placed in contact with the ATR crystal. Color image available online [Color figure can be viewed at wileyonlinelibrary.com]

Figure 5 shows the spectrum of each of the film samples where the laminated PCL film spectra were obtained for the PCL layer only.

The spectra of the SRC and SRC/NC films are similar. Broad peaks between $3,650$ and $3,200\text{ cm}^{-1}$ correspond to the hydroxyl groups of the SRC and bentonite clay, and the peaks between $3,000$ and $2,700\text{ cm}^{-1}$ are due to the alkane bonds of the SRC. Peaks at 844 , 930 , $1,035$, and $1,218\text{ cm}^{-1}$ are typical of the SRC functional groups of the C—O—SO₃ bonds of the d-galactose-4-sulfate, C—O of the 3,6-anhydro-d-galactose, the glycosidic linkage (C—O) of 3,6-anhydro-d-galactose, and the S=O bond of the sulfate ester, respectively.^[11] The typical bentonite clay peaks that are expected to appear at 660 , $1,450$, and $1,100$ – 800 cm^{-1} and are usually attributed to the Si—O—Si, Si—OH, and Al—O—Si bonds, respectively,^[60] are overlapped by the SRC bands. The PCL-laminated SRC and SRC/NC films exhibit almost exclusively the PCL vibrational peaks with the exception of there being a slight band corresponding to hydroxyl group absorption between $3,650$ and $3,200\text{ cm}^{-1}$ when compared with the neat PCL film. This may indicate there is no significant, or very little, diffusion between the SRC and PCL polymer molecules at the interface even though an interfacial interaction exists as suggested by the SEM cross-section analysis (see Figure 1a).

A very small band in the $3,650$ – $3,200\text{ cm}^{-1}$ region is noticeable in the spectrum of the PCL film that is associated with the hydroxyl group and which may be due to the hydrophobic character of the PCL layer. The other peaks occurring at $2,949$, $2,865$, $1,720$, $1,293$, $1,240$, and $1,170\text{ cm}^{-1}$ are attributed to common PCL characteristic stretching for asymmetric CH₂, symmetric CH₂, C=O, C—O, and C—C, asymmetric C—O—C, and symmetric C—O—C modes, respectively.^[61]

4 | CONCLUSIONS

Incorporating hydrophilic bentonite NC into SRC polymer film resulted in a general increase the mechanical properties, but with little or no improvement to the barrier properties. The latter is attributed to possible agglomeration of NC in the SRC matrix but more likely its hydrophilic nature that consequently impacts the water vapor barrier and water resistance. Laminating the SRC and SRC/NC films with PCL, however, increased the barrier properties of the film, compensating for the loss of these properties due to NC incorporation as well as further improved the mechanical properties. The thermal stability of the SRC film was improved by NC incorporation and PCL lamination with the combination of these

modifications resulting in the greatest improvement in the overall properties of the SRC film.

ORCID

Marlene J. Cran  <https://orcid.org/0000-0002-6000-8093>

REFERENCES

- [1] S. Pathak, C. L. R. Sneha, B. B. Mathew, *J. Polym. Biopolym. Phys. Chem.* **2014**, *2*, 84.
- [2] N. Blanco-Pascual, M. P. Montero, M. C. Gómez-Guillén, *Food Hydrocoll.* **2014**, *37*, 100.
- [3] W. M. Siah, A. Aminah, A. Ishak, *Int. Food Res. J.* **2015**, *22*, 2230.
- [4] G. A. Paula, N. M. B. Benevides, A. P. Cunha, A. V. de Oliveira, A. M. B. Pinto, J. P. S. Morais, H. M. C. Azeredo, *Food Hydrocoll.* **2015**, *47*, 140.
- [5] N. Rajendran, S. Puppala, S. M. Raj, R. B. Angeeleena, C. Rajam, *J. Pharm. Res.* **2012**, *5*, 1476.
- [6] S. Distantina, R. Rochmadi, M. Fahrurrozi, W. Wiratni, *Mod. Appl. Sci.* **2013**, *7*, 22.
- [7] L. Cunha, A. Grenha, *Mar. Drugs* **2016**, *14*, 42.
- [8] M. Karel, B. D. Lund, in *Physical Principles of Food Preservation* (Eds: O. R. Fennema, Y. H. Hui, M. Karel, P. W. J. R. Whitaker), Marcel Dekker, Inc., New York **2003**, Chapter 12, p. 514.
- [9] S. Zarina, I. Ahmad, *Bioresources* **2015**, *10*, 256.
- [10] R. E. Cian, P. R. Salgado, S. R. Drago, A. N. Mauri, *J. Appl. Phycol.* **2014**, *27*, 1699.
- [11] B. B. Sedayu, M. J. Cran, S. W. Bigger, *J. Polym. Environ.* **2018**, *26*, 3754.
- [12] T. Wittaya, in *In Structure and Function of Food Engineering* (Ed: A. A. Eissa), IntechOpen, London **2012**, Chapter 5, p. 103.
- [13] S. Shojae-Aliabadi, M. A. Mohammadifar, H. Hosseini, A. Mohammadi, M. Ghasemlou, S. M. Hosseini, M. Haghshenas, R. Khaksar, *Int. J. Biol. Macromol.* **2014**, *69*, 282.
- [14] J.-W. Rhim, L. F. Wang, *Carbohydr. Polym.* **2013**, *96*, 71.
- [15] L. R. Rane, N. R. Savadekar, P. G. Kadam, S. T. Mhaske, *J. Mater.* **2014**, *2014*, 1.
- [16] J.-W. Rhim, *Carbohydr. Polym.* **2011**, *86*, 691.
- [17] M. H. Gabr, N. T. Phong, M. A. Abdelkareem, K. Okubo, K. Uzawa, I. Kimpara, T. Fujii, *Cellulose* **2013**, *20*, 819.
- [18] J. T. Martins, A. I. Bourbon, A. C. Pinheiro, B. W. S. Souza, M. A. Cerqueira, A. A. Vicente, *Food Bioprocess Technol.* **2012**, *6*, 2081.
- [19] A. Sorrentino, G. Gorrasi, V. Vittoria, *Trends Food Sci. Technol.* **2007**, *18*, 84.
- [20] C. M. O. Müller, J. B. Laurindo, F. Yamashita, *Carbohydr. Polym.* **2012**, *89*, 504.
- [21] M. Avella, M. E. Errico, P. Laurienzo, E. Martuscelli, M. Raimo, R. Rimedio, *Polymer* **2000**, *41*, 3875.
- [22] L. Sánchez-González, M. Vargas, C. González-Martínez, A. Chiralt, M. Cháfer, *Food Hydrocoll.* **2009**, *23*, 2102.
- [23] S. Shojae-Aliabadi, H. Hosseini, M. A. Mohammadifar, A. Mohammadi, M. Ghasemlou, S. M. Hosseini, R. Khaksar, *Carbohydr. Polym.* **2014**, *101*, 582.
- [24] N. F. N. Rekeem, N. H. Z. Abedin, *Carbohydr. Polym.* **2017**, *157*, 1479.
- [25] A. R. V. Ferreira, V. D. Alves, I. M. Coelho, *Membranes* **2016**, *6*, 22.
- [26] J.-W. Rhim, K. A. Mohanty, S. P. Singh, P. K. W. Ng, *Ind. Eng. Chem. Res.* **2006**, *45*, 3059.
- [27] S.-I. Hong, J. M. Krochta, *J. Food Sci.* **2003**, *68*, 224.
- [28] K. Khwaldia, E. Arab-Tehrany, S. Desobry, *Comp. Rev. Food Sci. Food Safety* **2010**, *9*, 82.
- [29] O. Myllymaki, P. Myllarinen, P. Forsell, T. Suortti, K. Lahteenkorva, R. Ahvenainen, K. Poutanen, *Packag. Technol. Sci.* **1998**, *11*, 265.
- [30] F. Tihminlioglu, İ. D. Atik, B. Özen, *J. Food Eng.* **2010**, *96*, 342.
- [31] M. Yasin, B. J. Tighe, *Biomaterials* **1992**, *13*, 9.
- [32] R. Ortega-Toro, S. Collazo-Bigliardi, P. Talens, A. Chiralt, *J. Appl. Polym. Sci.* **2016**, *133*, 42220.
- [33] M. A. T. Duarte, R. G. Hugen, E. S. A. Martins, A. P. T. Pezzin, S. H. Pezzin, *Mater. Res.* **2006**, *9*, 25.
- [34] M. F. Koenig, S. J. Huang, *Polymer* **1995**, *36*, 1877.
- [35] O. O. Fabunmi, L. G. Tabil, S. Panigrahi, P. R. Chang, *J. Polym. Environ.* **2011**, *19*, 841.
- [36] R. Ortega-Toro, A. Muñoz, P. Talens, A. Chiralt, *Food Hydrocoll.* **2016**, *56*, 9.
- [37] G. O. Phillips, in *In Gums and Stabilisers for the Food Industry* (Eds: G. O. Phillips, P. A. Williams, D. J. Wetlock), Oxford University Press, Oxford **1996**, Chapter 8, p. 403.
- [38] J.-W. Rhim, *Food Res. Int.* **2013**, *51*, 714.
- [39] A. Farhan, N. M. Hani, *Food Hydrocoll.* **2017**, *64*, 48.
- [40] P. J. A. Sobral, F. C. Menegalli, M. D. Hubinger, M. A. Roques, *Food Hydrocoll.* **2001**, *15*, 423.
- [41] ASTM D882-18, Standard Test Method for Tensile Properties of Thin Plastic Sheeting, ASTM International, West Conshohocken, PA, **2018**. www.astm.org
- [42] J. Gómez-Estaca, B. Giménez, P. Montero, M. C. Gómez-Guillén, *J. Food Eng.* **2009**, *92*, 78.
- [43] T. Honma, T. Senda, Y. Inoue, *Polym. Int.* **2003**, *52*, 1839.
- [44] C. C. Eng, N. A. Ibrahim, N. Zainuddin, H. Ariffin, W. M. Z. W. Yunus, Y. Y. Then, C. C. Teh, *Indian J. Mater. Sci.* **2013**, *2013*, 11.
- [45] J.-W. Rhim, L. F. Wang, *Appl. Clay Sci.* **2014**, *97-98*, 174.
- [46] M. Alboofetileh, M. Rezaei, H. Hosseini, M. Abdollahi, *J. Food Eng.* **2013**, *117*, 26.
- [47] R. Sothornvit, S.-I. Hong, D. J. An, J.-W. Rhim, *LWT-Food Sci. Technol.* **2010**, *43*, 279.
- [48] F. Masarin, F. R. P. Cedeno, E. G. S. Chavez, L. E. de Oliveira, V. C. Gelli, R. Monti, *Biotechnol. Biofuels* **2016**, *9*, 122.
- [49] U. Siripatrawan, B. R. Harte, *Food Hydrocoll.* **2010**, *24*, 770.
- [50] M. A. Cerqueira, B. W. S. Souza, J. A. Teixeira, A. A. Vicente, *Food Hydrocoll.* **2012**, *27*, 175.
- [51] C. M. O. Müller, J. B. Laurindo, F. Yamashita, *Ind. Crop Prod.* **2011**, *33*, 605.
- [52] T. P. Labuza, C. R. Hyman, *Trends Food Sci. Technol.* **1998**, *9*, 47.
- [53] A. Mahieu, C. Terrie, N. Leblanc, *Packag. Res.* **2017**, *2*, 1.
- [54] H. Almasi, B. Ghanbarzadeh, A. A. Entezami, *Int. J. Biol. Macromol.* **2010**, *46*, 1.
- [55] M. Alexandre, P. Dubois, *Mater. Res. Eng. Rep.* **2000**, *28*, 1.
- [56] A. M. Nafchi, R. Nassiri, S. Sheibani, F. Ariffin, A. A. Karim, *Carbohydr. Polym.* **2013**, *96*, 233.
- [57] S. L. M. El Halal, G. P. Bruni, J. A. do Evangelho, B. Biduski, F. T. Silva, A. R. G. Dias, E. da Rosa Zavareze, M. de Mello Luvielmo, *Starch Stärke* **2018**, *70*, 1700115.
- [58] F. A. Aouada, L. H. C. Mattoso, E. Longo, *Ind. Crop Prod.* **2011**, *34*, 1502.
- [59] P. Kumar, K. P. Sandeep, S. Alavi, V. D. Truong, R. E. Gorga, *J. Food Eng.* **2010**, *100*, 480.
- [60] T. G. Almeida, A. R. M. Costa, R. M. R. Wellen, E. L. Canedo, L. H. Carvalho, *Mater. Res.* **2017**, *20*, 1503.

[61] G. Janarthanan, I. G. Kim, E.-J. Chung, I. Noh, *Biomater. Res.* **2019**, *23*, 1.

SUPPORTING INFORMATION

Additional supporting information may be found online in the Supporting Information section at the end of this article.

How to cite this article: Sedayu BB, Cran MJ, Bigger SW. Improving the moisture barrier and mechanical properties of semi-refined carrageenan films. *J Appl Polym Sci.* 2020;137:e49238. <https://doi.org/10.1002/app.49238>